

## Computer vision based interface level control in a separation cell

Phanindra Jampana\* Sirish Shah\* Ramesh Kadali\*\*  
Dejan Kihass\*\*\*

\* Department of chemical engineering, University of Alberta,  
Edmonton, AB T6G2E1, Canada (e-mail: pjampana@ualberta.ca,  
slshah@ualberta.ca).

\*\* Suncor Energy Inc., Fort McMurray, AB T9H3E3, Canada (e-mail:  
rkadali@suncor.com)

\*\*\* Matrikon Inc., Edmonton, AB T5J3N4, Canada (e-mail:  
dejan.kihass@matrikon.com)

---

**Abstract:** Bitumen extraction from oil sands is the core process in the production of oil from oil sands. This floatation process is carried out in large vessels called separation cells. Optimal control of the interface between Bitumen froth and Middlings in these cells can result in a significant improvement in Bitumen recovery and increase process efficiency downstream, resulting in large economic benefits. The major impediment in the implementation of such a control system is the lack of safe and reliable sensors for interface level detection. Traditional instruments such as nuclear gauges, capacity probes etc. are either unsafe or do not give reliable estimates. This work describes a novel sensor for interface level detection, developed using computer vision techniques on video frames captured from a sight glass camera. Specifically, State-space model based Particle filtering is used to provide estimates of the interface level and its quality. It is shown that the algorithm is robust to lighting changes and process abnormalities. Industrial results show highly improved control performance when estimates of the sensor are used for feedback control.

---

### 1. INTRODUCTION

The Athabasca oil sands reserve in Alberta, Canada is the second largest oil reserve in the world [Govt.of.Alberta, 2007]. Crude oil extraction from oil sands is a billion dollar industry and currently it accounts for almost half of total crude oil production in Canada and 10% of North American oil production [Govt.of.Alberta, 2007].

The oil sands are a mixture of Sand, Clay, Water and Bitumen. Bitumen is extracted from these sands using a Water Based Extraction Process(WBEP), which is carried out in separation cells. Typically three layers form as shown in Fig.1. Of particular interest is the interface level

between the Bitumen-froth and the Middlings layer, which is known to affect the froth quality and Bitumen recovery and thus heavily influence process economics. For example, when this level is too high, fines (fine sand particles) escape into Bitumen-froth degrading its quality and when it is too low, Bitumen is lost to the Tailings ponds causing environmental problems. A good regulation of the interface level also reduces the variability of the process downstream and leads to optimal operating conditions[Jain, 2006]. Hence, there has been much interest in the oil sands industry to control this interface at an optimum level for Bitumen recovery.

The problem in implementing an automatic control system is the lack of safe and reliable instruments for interface level measurements. Traditional instruments such as Pressure transducers and Capacitance probes give very low resolution and unreliable estimates. Other expensive sensors such as Nuclear density profilers were abandoned because of issues of concern over their safety.

In the absence of precise interface level estimates, the interface level is currently controlled using low resolution Capacitance probe measurements. As these measurements are not accurate, operators frequently watch the sight glass video and adjust the interface level set point manually. The changes in the set point are done so as to negate the effect of inaccuracies in the Capacitance probe measurements. A typical image from such a video sequence observed by the operators is shown in Fig.2.

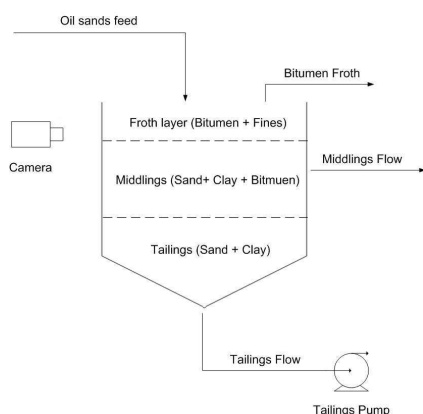


Fig.1. Separation cell

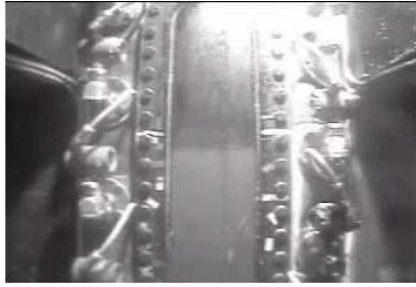


Fig.2. Sight view glass showing the interface between the Bitumen froth(dark surface) and the Middlings(light surface)

A novel idea to improve the accuracy of interface level measurements, is to detect the interface level by vision methods on video obtained from the sight glass video camera. The schematic in Fig 3 gives a birds eye view of the desired control system. The interface level estimated from the camera video is transmitted to the Distributed Control System (DCS) which in turn manipulates the pump speed to maintain the interface level at a given set point. The Application server hosts the automatic level detection program (vision sensor) and the Control room monitor displays the video images (shown in Fig.2) for the operators.

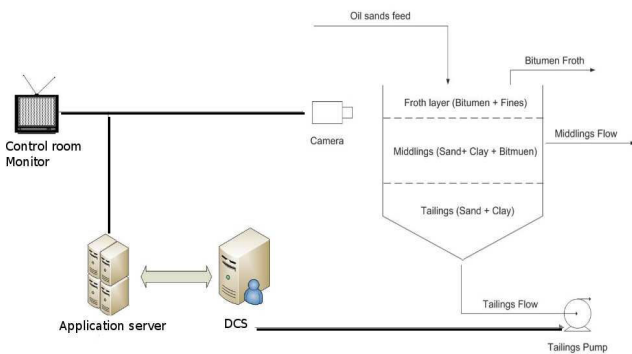


Fig.3. Overall schematic

The problem of interface level detection is a special case of a general problem of contour tracking, with the contour being approximated by a horizontal line. Contour tracking has been studied extensively in computer vision literature [Blake and Isard, 2000, Isard and Blake, 1998]. The methods studied there represent the contour by a parametric B-spline and use the Particle filtering algorithm to estimate the future values of these parameters based on observations collected from images and a State space model over the parameters. Particle filtering [Arulampalam et al., 2002, Doucet et al., 2001] is used because of its ability to maintain multiple hypothesis, i.e. being able to handle non-Gaussian type of state as well as measurement noise.

The current work is based on similar but simpler grounds. Bitumen-froth and Middlings interface is parametrized by a single scalar level value instead of a B-spline and the state model used for the interface is a simple random walk. For modelling edge observations extracted from the images, the model described in [Isard and Blake, 1998] is used. The output of the designed filter is a (posterior)

probability distribution of the interface level and the desired interface level value is then estimated from first order statistics of this distribution.

The main contributions of this paper are twofold:

- (1) Development of a particle filter based vision sensor for interface level detection and
- (2) Use of this sensor in a feed back loop for maintaining the interface at a desired level for optimum Bitumen recovery

The rest of the paper is organized as follows: Section 2 discusses the Particle filter along with the core algorithm used in this paper. Section 3 shows the simple image processing steps performed and the extraction of salient edge features. The state and observation models for interface level detection are developed in section 4. Section 5 focuses on the implementation aspects of the Particle filter and also discusses the quality estimation step. Section 6 presents the results followed by concluding remarks in section 7.

## 2. PARTICLE FILTERS

Consider the following discrete time state space model:-

$$x_k = f(x_{k-1}) + w_{k-1} \quad (1)$$

$$z_k = g(x_k) + v_k \quad (2)$$

where  $w$  and  $v$  are random processes representing state and measurement noises respectively and whose statistics are assumed to be known. The aim of filtering is to estimate the following *posterior* distribution

$$p(x_k | z_1, z_2, \dots, z_k) \quad (3)$$

The posterior distribution contains all the information about the state  $x_k$  that can possibly be obtained from the set of noisy measurements  $z_1, z_2, \dots, z_k$ . Any estimate of the state  $x_k$  can be obtained (e.g. mean or mode estimate) once this distribution is known. For real time implementation of the algorithm it is important that the posterior distribution be computed recursively. The following assumptions are made for recursive estimation :

$$p(x_k | x_1, x_2, \dots, x_{k-1}) = p(x_k | x_{k-1}) \quad (4)$$

$$p(z_1, z_2, \dots, z_k | x_1, x_2, \dots, x_k) = \prod_{i=1}^k p(z_i | x_1, x_2, \dots, x_k) \quad (5)$$

Based on the assumptions above the following can be derived using Bayes theorem:

$$p(x_k | z_1, z_2, \dots, z_k) \propto p(z_k | x_k) p(x_k | z_1, z_2, \dots, z_{k-1}) \quad (6)$$

This equation is expressed as

$$\text{posterior} \propto \text{likelihood} * \text{prior} \quad (7)$$

The *prior* is the information about the state *before* the arrival of the new observation  $z_k$ . The observation  $z_k$  updates the prior through the likelihood function resulting in the posterior. It is to be noted that if the mappings  $f$  and  $g$  are linear and the state/measurement noises are Gaussian, the prior and the posterior distributions are also Gaussian and hence characterized only by their first and second

moments(mean and variance). In such cases, the analytical recursive solution for the mean and variance is given by the Kalman filter algorithm. In the general case (linear or nonlinear systems affected by non-Gaussian noise processes), the distributions cannot be evaluated analytically and Monte Carlo simulation methods are resorted to. Also, the recursive nature of (6) makes it possible to estimate these distributions sequentially. These methods are called sequential Monte Carlo methods or particle filters. One such method used frequently is the Sampling Importance Resampling (SIR) algorithm described below:-

*Sampling Importance Resampling(SIR) algorithm*

SIR is a Monte Carlo technique used to generate samples from distributions which are difficult to sample from and which are known only up to a proportionality constant. Let  $p(y)$  be such a distribution. Consider any (importance) distribution  $q(y)$  which is easy to sample from and generate the samples  $[y_1, y_2, \dots, y_N]$ . Compute the weights  $w_i = \frac{p(y_i)}{q(y_i)}$  and sample from the discrete distribution which places weights  $w_i$  at  $y_i$  N times. It can be shown that as  $N \rightarrow \infty$  the discrete distribution tends to the original distribution  $p(y)$ [Fearnhead, 1998]. Hence the N samples represent samples(particles) from  $p(y)$ . If the prior is assumed to be the importance density and we desire to generate samples from the posterior, from (6) it can be seen that the weights are given by  $p(z_k|x_k^i)$ , where  $x_k^i$  represent samples from the prior. These prior samples are generated by passing the samples from the posterior at the previous time step through the state equation. This is described in the complete SIR algorithm below:

- 
- Assume  $[x_{k-1}^i; i = 1 : N]$  are generated from  $p(x_{k-1}|z_1, z_2, \dots, z_{k-1})$
  - Generate samples  $[x_{k|k-1}^i; i = 1 : N]$  by  $x_{k|k-1}^i = f(x_{k-1}^i) + w_{k-1}$ . These represent samples from the prior  $p(x_k|z_1, z_2, \dots, z_{k-1})$
  - Calculate the weights  $p(z_k|x_k = x_{k|k-1}^i)$
  - Resample from the discrete distribution which places the weights  $p(z_k|x_k = x_{k|k-1}^i)$  at  $x_{k|k-1}^i$ , these represent samples from  $p(x_k|z_1, z_2, \dots, z_k)$
- 

As  $p(x_0)$  is known the assumption in step one is valid for the first iteration and hence all the posterior distributions can be computed recursively.

3. EDGE FEATURE EXTRACTION

Edge features are extracted from the input images using simple image processing techniques. Initially, the region is smoothed using a Gaussian 3x3 kernel of variance 0.5. Horizontal edge detection is then performed on the smoothed image using the simple mask  $[-1 \ 0 \ 1]^T$ . From the resulting image the strongest  $M$  pixels in each column are selected. A sample transformation of the image in Fig.2 is shown in Fig.4 (with  $M = 5$ ).

There are two main reasons for adopting the procedure above instead of thresholding the edge image

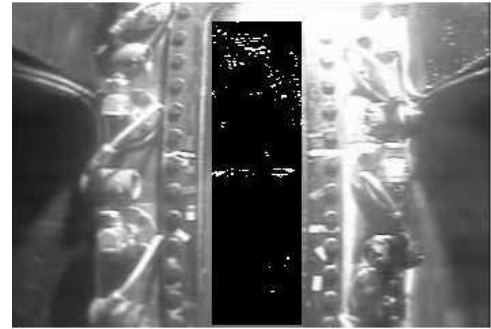


Fig.4. Edge image (based on transformation of the image shown in Fig.2)

- Choosing a hard threshold for edge detection can result in the algorithm being susceptible to lighting changes
- With a hard threshold, the number of edge points in each column would not be constant and hence the likelihood model  $p(z_k|x_k)$  will not be known before  $z_k$  is observed (c.f Section 4)

4. STATE AND OBSERVATION MODELS

4.1 State model

Modelling the dynamics of the Bitumen-froth and Middlings interface from first principles is difficult because it is governed by several complex physical and chemical interactions between Bitumen, Sand, Clay, Water and reagents (e.g. Caustic is added to hasten the separation process) as well as flow rates of process utilities like hot water. In addition to these complexities, the addition of feed from the top of the cell causes a slushing effect inside the separation cell resulting in very fast dynamics. In fact, this phenomenon is the main contributor to the observed dynamics of the Bitumen-froth and Middlings interface. Unfortunately, this slushing effect cannot be modelled satisfactorily. Thus, even empirical laws for interface level dynamics (based on feed quality and input, output flow rates of all streams) cannot be reliably estimated. Hence, the interface level dynamics is modelled as a simple random walk process:

$$x_k = x_{k-1} + w_k \tag{8}$$

where  $x_k$  represents the interface level at time  $k$ .  $w_k$  represents a Gaussian process with a small variance  $\gamma^2$ . A justification of the model is based on:

- (1) Temporal continuity - the fact that level at time  $k$  would not be very different from level at time  $k - 1$  especially if the frame rate of the camera is as high as 30fps.
- (2) Level dynamics of a pumped tank are captured by an integrating process

4.2 Observation model

To form the observation model, the edge image obtained after the image processing described above is transformed into an observation vector  $z_k$ . This is done as follows: let  $z_{k_i}$  represent the vector of  $M$  measurements obtained from

the  $i^{th}$  column of the edge image, where the elements of  $z_{k_i}$  are the heights of the edge points (from the base of the image) in that column. Then the overall  $z_k$  is constructed by stacking all  $z_{k_i}$  i.e.  $z_k = [z_{k_1}, z_{k_2}, \dots, z_{k_C}]^T$  where  $C$  represents the total number of columns in the edge image, so the dimension of  $z_k$  is  $MC$ . In the case of perfect measurements (i.e. no noise in the edge image) and with  $M = 1$  all the elements of  $z_k$  will be equal to  $x_k$  for a one pixel thick edge. So, in the presence of noise  $v_k$ , the observations can be modelled as:-

$$z_k = 1_{MC}x_k + v_k \quad (9)$$

where  $1_{MC}$  represents a vector of ones of dimension  $MC$ . The measurement noise model  $p(v_k)$  is the same as  $p(z_k|x_k)$  except for a mean value (from (9)). The choice of  $p(z_k|x_k)$  is the most crucial step and it has been found that if it is taken to be a Gaussian density, the filter is caught between the noise and the actual interface level. This is because uni-modal densities cannot represent the type of noise observed in Fig 3. The non-Gaussian likelihood described in [Isard and Blake, 1998] can be chosen for this purpose:

$$p(z_k|x_k) = p(z_{k_1}, z_{k_2}, \dots, z_{k_C}|x_k) \quad (10)$$

$$= \prod_{j=1}^C p(z_{k_j}|x_k) \quad (11)$$

$$= \prod_{j=1}^C \left(1 + \sum_{i=1}^M \exp(-(z_{k_j}^i - x_k)^2/\sigma^2)\right) \quad (12)$$

where  $z_{k_j}^i$  represents the elements of  $z_{k_j}$  and  $\sigma^2$  is akin to the measurement noise variance. The assumption here is that the edge points in each column are independent of each other given the level. Other likelihood functions which are not bound to this assumption can be used, e.g.

$$p(z_k|x_k) = p(z_{k_1}, z_{k_2}, \dots, z_{k_C}|x_k) \quad (13)$$

$$= \sum_{j=1}^C p(z_{k_j}|x_k) \quad (14)$$

$$= \sum_{j=1}^C \sum_{i=1}^M \exp(-(z_{k_j}^i - x_k)^2/\sigma^2) \quad (15)$$

which gives a high likelihood to the state ( $x_k$ ) which minimizes the sum of the distances between the edge points observed and  $x_k$ , but it has not been found to give any significant improvement to the algorithm. So, the likelihood function (12) is used here. When this likelihood function is observed as a function in  $x_k$  rather than  $z_k$ , it can be seen that the peaks of the function will be located at  $z_{k_j}^i$ , this makes the likelihood function multi-modal. As noted earlier such a likelihood function is essential for robust tracking as it can handle more general types of noise distributions. The value of  $M$  reflects the thickness of the interface (edge), the model (9) gives good results only for medium values of  $M$ , typically 3-6. If  $M$  is too small, only noise may be captured in the measurements and if  $M$  is too high the edge image contains too many spurious edges and the filter will be confused in both the cases. A value of  $M = 5$  has been found to give good results.

Using the state and observation models described above, the basic particle filter obtained is demonstrated in Fig.5. In each of the two frames, the posterior probability density is shown on the left and the extracted edges are shown on the right. The posterior density is multimodal in the left frame, owing to the large extent of spurious edges present on the top part of the edge image. As new images are obtained in time, the filter rejects the spurious peak in favour of the actual interface as shown in the right frame.

## 5. IMPLEMENTATION ISSUES

The particle filter is initialized by modelling  $p(x_0)$  as a uniform distribution between the upper and lower limits of the view glass area.  $P = 300$  particles are generated from this distribution and subsequently updated according to the SIR filtering algorithm shown earlier using the state and observation models in (8) and (9). With the parameters  $\gamma = 3$  pixels,  $\sigma = 5$  pixels the particle filter is able to track the interface level quite well under normal operating conditions.

To handle process abnormalities, a quality estimate of the input image is also computed. This estimate is used, for example, to switch to manual control when the quality is bad for a sustained period of time. Two cases where the quality estimate is useful are:

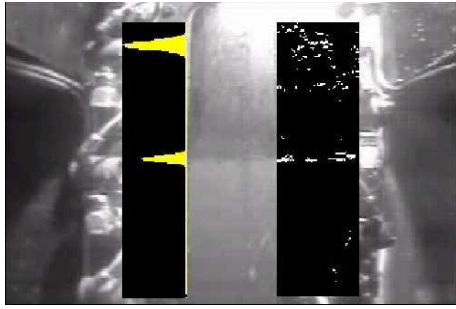
- (1) The interface between Bitumen-froth and Middlings layers is blurry.
- (2) The interface is not visible in the image because it is above or below the sight view glass area

The quality estimate is computed in a straight forward way by considering the support of the posterior p.d.f. Under normal operating conditions (with clear interface) the particles are a maximum of 6 – 9 pixels apart and this support increases as the interface becomes blurry. Hence, there is a direct correlation between visual quality of the interface and the support of the posterior p.d.f. This is shown more clearly in Fig.8. A threshold of 15 pixels on the support is used currently to distinguish between the bad (quality = 0) and good (quality = 1) quality input images. To avoid cases where the interface level is not present in the view glass area, alarms are announced whenever the interface level crosses 10% and 90% bounds for operator intervention.

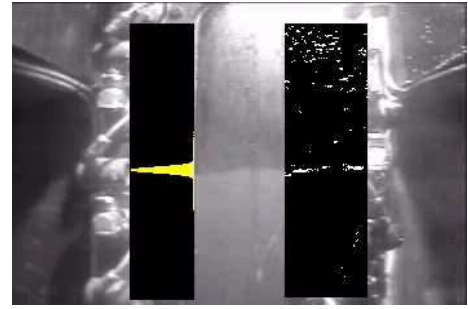
The final algorithm operates at 9fps and these filter outputs are averaged over one second and communicated to the Distributed Control System (DCS). The software used for image processing is Intel Integrated Performance Primitives for Windows 5.1 and OpenCV is used for display purposes. Matrox Meteor II frame grabber card is used for image transfer from the analog camera to the PC.

## 6. RESULTS

Fig 6. shows the output of the filter on good quality frames from a video sequence. The black line superimposed on the image is the mode of the posterior probability density function. For each image the support of the posterior distribution is also given. Fig 7 shows frames along with the edges detected. Note that even though there are

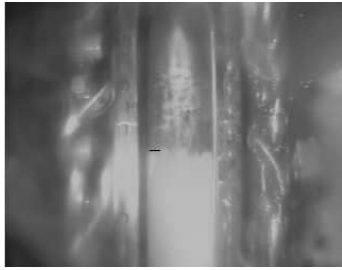


Second Frame

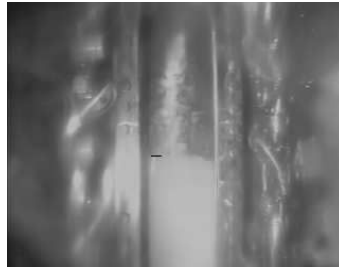


A later Frame

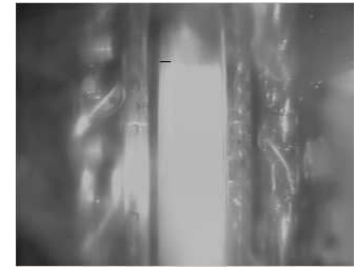
Fig.5. Two frames from a tracked video sequence



Support = 7 pixels



Support = 8 pixels



Support = 8 pixels

Fig.6. Tracker output on good quality frames.



Fig.7. Edge Images. The white pixels are the strongest edges detected in each column

spurious edges the filter is able to detect the interface very well.

Fig 8. shows frames with changed lighting conditions. In these frames the posterior probability distribution is also shown next to the superimposed line. In all these frames the support very closely reflects the visual quality of the interface. The last frame in this figure is an example of a bad quality interface (support greater than 15 pixels). Support of the posterior p.d.f is dependant not only on the current video frame but also on  $\sigma$  and  $\gamma$ . Increase in any of these increases the support but also affects the robustness of the filter. In the last frame of Fig.8 the support is smaller than what can be observed visually because of the particular choice of  $\sigma$  and  $\gamma$  which tries to maintain robustness of the filter.

Fig.9 highlights the stability of the filter. For example, in the first frame three interfaces are visible but because of the temporal continuity constraint in the state model, the filter is undisturbed. The second frame highlights a similar concept in the case of partial obstruction of camera view.

Fig 10. compares results when estimates from the Capacitance probe and the current image based sensor are used

in closed loop control of the interface level. The figure on the left shows the control achieved with the Capacitance probe measurements (and the manual set point changes by the operators) whereas the figure on the right shows the control achieved by the vision based sensor. From the descriptive fifteen hour time trend shown on the left it can be seen that the variance in the interface level and the pump speed is clearly very high. Note that there is no unique interface level set point shown as it is constantly manipulated by the operators. With the control based on the vision sensor however, the interface level closely follows the set point (Note the change in scale in the y axis). This interface level is also not affected by rapid feed surges and the pump speed is also relatively constant, pointing to a smooth operation of the control system.

Finally, using approximately three weeks of laboratory data (one week of camera control, two weeks of Capacitance probe control), it has been calculated that the Bitumen losses in Tailings dropped by 53.6%. A similar reduction of 29.12% has also been noticed in Bitumen losses to Middlings. The laboratory data indicates increased economic benefit and reduced environmental losses. Process data collected for the same duration also indicated signifi-

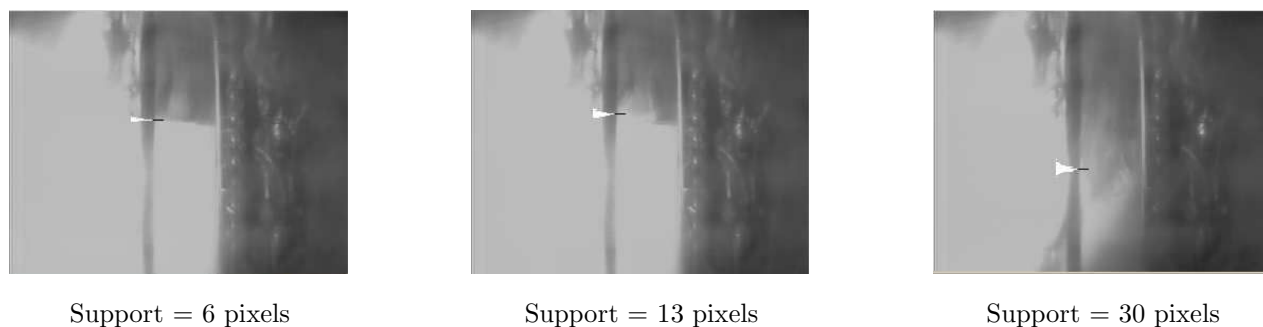
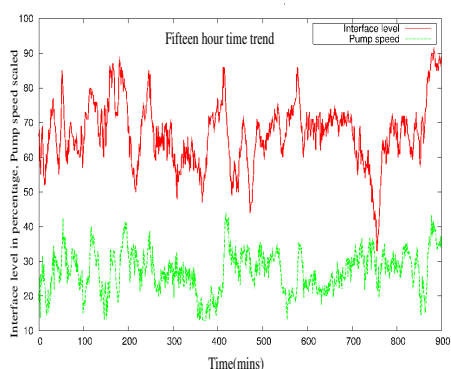


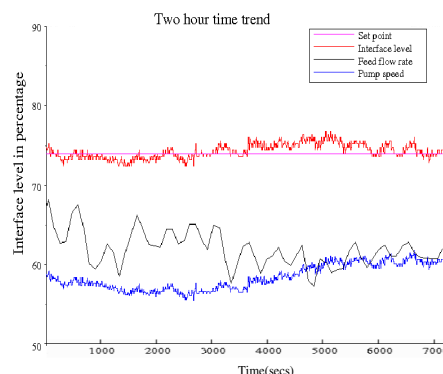
Fig.8. Change of lighting conditions



Fig.9. Stability of the filter



Partial manual control



Automatic control using vision sensor

Fig.10. Closed loop control results

cant reduction in the variance of process variables around the separation cell (Interface level, Tailings pump speed, Tailings flow rate, Froth temperature, etc.) resulting in a steadier process operation benefiting the downstream processes. Plant personnel attribute the gains to tighter control achievable using the interface level obtained from the camera images and the feed forward component used in the controller.

## 7. ACKNOWLEDGEMENTS

The authors would like to thank Dr. Syed Imtiaz and Dr. Kallol Roy for their help on Particle Filters. Financial support from NSERC, Matrikon, Suncor and iCORE in the form of the Industrial Research Chair(IRC) program at the University of Alberta is gratefully acknowledged.

## REFERENCES

- S. Arulampalam, S. Maskell, N. J. Gordon, and T. Clapp. A tutorial on particle filters for on-line non-linear/non-gaussian bayesian tracking. *IEEE Transactions of Signal Processing*, 50:174 – 188, 2002.
- A. Blake and M. Isard. *Active contours*. Springer, 2000.
- A. Doucet, N. de Freitas, and N. Gordon. *Sequential Monte Carlo Methods in Practice*. Springer, 2001.
- Paul Fearnhead. *Sequential Monte Carlo methods in filter theory*. PhD thesis, University of Oxford, 1998.
- Govt.of.Alberta. Alberta energy: Oil sands, 2007. URL [www.energy.gov.ab.ca/OurBusiness/oilsands.asp](http://www.energy.gov.ab.ca/OurBusiness/oilsands.asp).
- M. Isard and A. Blake. Condensation - conditional density propagation for visual tracking. *International Journal of Computer Vision*, 29:5 – 28, 1998.
- Mridul Jain. Practical issues in performance control monitoring. Master's thesis, University of Alberta, 2006.